OncoTargets and Therapy

Dovepress
Taylor & Francis Group

Open Access Full Text Article

ORIGINAL RESEARCH

The Dual Role of RBBP7 in Esophageal Squamous Cell Carcinoma: Cell Context-Dependent Impacts on Proliferation and Radiosensitivity

Yafen Li[1,2,*], Shuai Lu[3,*], Hui Yao[1], Genbao Zhu[2], Hao Liu[4], Zhiyu Ma[5], Heng Tang[2]

[1]Department of Clinical Pharmacy, Wanbei Coal and Electricity Group General Hospital, Suzhou, Anhui, People's Republic of China; [2]General Clinical Research Center, Wanbei Coal and Electricity Group General Hospital, Suzhou, Anhui, People's Republic of China; [3]Department of Joint, Wanbei Coal and Electricity Group General Hospital, Suzhou, Anhui, People's Republic of China; [4]Department of Radiology, Wanbei Coal and Electricity Group General Hospital, Suzhou, Anhui, People's Republic of China; [5]Department of Radiotherapy, Wanbei Coal and Electricity Group General Hospital, Suzhou, Anhui, People's Republic of China

*These authors contributed equally to this work

Correspondence: Heng Tang; Zhiyu Ma, Email Tangheng@mail.ustc.edu.cn; mazhiyu02@sina.com

Background: Radiotherapy resistance contributes to poor prognosis in esophageal squamous cell carcinoma (ESCC). Retinoblastoma-binding protein 7 (RBBP7) is a nuclear protein, and it can promote or inhibit tumor progression in cancer, but its function in ESCC cells and impact on radiosensitivity remains unclear.

Methods: RBBP7 expression in cancer was analyzed using an online website. The expression levels of RBBP7 in ESCC cells (TE-1 and KYSE-150) and tissues were tested. Cells were subjected to RBBP7 gene silencing and irradiation (IR). Assays included CCK-8, clonogenic survival, flow cytometry (apoptosis/cell cycle), ROS detection, and Western blotting for DNA damage (γ-H2AX) and STAT3 signaling. Additionally, pathological tissue specimens and clinical data from ESCC patients were used to explore the expression of RBBP7.and its relationship with the clinical parameters of patients.

Results: RBBP7 was overexpressed in malignant tumors. In ESCC cells, the mRNA and protein of RBBP7 were also highly expressed. After silencing RBBP7 combined with IR treatment, contradictory effects were observed between cell lines: In well-differentiated TE-1 cells, RBBP7 knockdown suppressed proliferation, enhanced radiosensitivity (SER=1.370), increased ROS/DNA damage (γ-H2AX), promoted apoptosis, and reduced STAT3 activation (possibly through STAT3 signaling). In poorly-differentiated KYSE-150 cells, knockdown promoted proliferation, decreased radiosensitivity (SER=0.775), reduced apoptosis, and increased p-STAT3. In addition, knockdown caused S-phase arrest (TE-1) versus G0/G1 arrest (KYSE-150), with divergent CDK4/Cyclin D1 regulation. Clinical analysis confirmed RBBP7 positivity correlated with tumor differentiation, TNM stage, and radiotherapy method.

Conclusion: RBBP7 is highly expressed in ESCC, and it exerts cell context-dependent dual roles in ESCC, leading to differences in cellular radiosensitivity, possibly mediated through STAT3 signaling. This dichotomy highlights its potential as a differentiation status-specific therapeutic target.

Keywords: esophageal squamous cell carcinoma, RBBP7, radiosensitivity, STAT3, TNM staging

Introduction

Esophageal cancer (EC) is a common clinical malignancy of the digestive tract and is among the top ten new cancers worldwide. According to a statistical analysis of global cancer, there were more than 510,000 new cases of EC and 440,000 deaths worldwide in 2022; new cases accounted for 2.6% of all ECs, and deaths accounted for 4.6%,[1] reflecting the high mortality in EC. Pathologically, ESCC is the predominant type in Asian countries, constituting over 90% of cases.[2] ESCC patients often experience rapid disease progression and are unable to undergo surgical resection due to the absence of apparent early symptoms and effective screening methods. Therefore, Chemoradiotherapy is a prevalent treatment option for patients with ESCC. Nevertheless, most patients with ESCC do not show an adequate response to

Received: 21 April 2025
Accepted: 4 August 2025
Published: 4 September 2025

treatment and tumor radioresistance can lead to tumor recurrence, the prognosis remains unfavorable.[3] Thus, identifying biomarkers to overcome radioresistance is imperative for improving ESCC prognosis.

RBBP7, also known as retinoblastoma-protein associated 46 (RbAp46), belongs to the retinoblastoma protein (RB) family and is highly homologous to RBBP4.[4] It is a chromatin remodeler in HDAC complexes, RBBP7 promotes histone deacetylation and subsequent transcriptional repression, In the B-type histone acetyltransferase complex, RBBP7 is required for chromatin assembly after DNA replication.[5] The role of RBBP7 in malignancies is complex, and research has demonstrated that RBBP7 overexpression can enhance stress-induced apoptosis and inhibit growth in cervical cancer cells,[6] it can suppresses breast cancer progression via apoptosis induction.[7,8] However, RBBP7 can induce epithelial-mesenchymal transition, thereby contributing to cancer progression and metastasis.[9] In addition, Prior studies report conflicting roles: knockdown of RBBP7 in ESCC cells did not affect tumor apoptosis or tumor growth. However, the overexpression of RBBP7 significantly enhanced the invasion and migration of ESCC cells.[10] Critically, there are limited studies on the role of RBBP7 in ESCC - particularly regarding radiotherapy response - needs to be further studied.

Beyond general chromatin regulation, RBBP7 may directly influence radiosensitivity through: RBBP7 interacts with RB to participate in cell cycle regulation. In the G0/G1 phase, they inhibit gene expression regulated by E2F family transcription factors, thereby preventing cells from entering the S phase.[11] Additionally, the absence of RBBP7 can cause cells to be arrested in the G2/M phase and can also regulate mitosis by ubiquitin-dependent loading of centromere protein A (CENP-A) synthesized in the G1 phase.[12] Dysregulation could impair radiation-induced cell cycle arrest, a determinant of radioresponse.[13] Critically, RB is not only regulated by RBBP7 but also targeted by STAT3. RB, as a downstream substrate of CDK4/6, serves as a critical regulator of the G1-to-S phase transition. Its activity is modulated by both c-Myc and p53. STAT3 has been demonstrated to induce RB protein degradation via upregulation of c-MYC, thereby conferring resistance to CDK4/6 inhibitors.[14,15]

The signal transducer and activator of transcription 3 (STAT3) is a research hotspot in the field of cancer, serves as an essential nuclear transcription factor, it can form dimers that translocate into the nucleus to bind with DNA and then regulate gene transcription and cellular signal transduction.[16] As the convergence point of multiple tumor pathways, it can promote tumor cell proliferation, and anti-apoptosis, mediate carcinogenic inflammation and inhibit anti-tumor immunity when expressed in a large number of tumor cells. STAT3 is also considered a key gene for radiosensitivity, and Wang et al[17] illustrated that (MicroRNA-124) miR-124 can sensitize cancer patients during radiotherapy through STAT3. STAT3 inhibitor, stattic, can reverse the radioresistance of ESCC by inhibiting the activation of STAT3 and the expression of hypoxia-inducible factor-1 (HIF-1α) and vascular endothelial growth factor (VEGF).[18] As a histone chaperone, RBBP7 may alter chromatin accessibility at STAT3 target genes, providing a direct epigenetic link between RBBP7 and STAT3-driven radioresistance. Supporting this, HIF-1α upregulates the expression of RBBP7 under hypoxic conditions,[13] implying crosstalk with radioresistance pathways.

Given RBBP7's context-dependent duality,[10] we hypothesized that its impact on ESCC radiosensitivity varies with tumor differentiation status. We selected two ESCC lines: TE-1 (well-differentiated) and KYSE-150 (poorly-differentiated). This study will explore the effects of RBBP7 on ESCC and its influence on radio-sensitization through in vitro cell experiments.

Materials and Methods

Cell Culture and Intervention

Human ESCC lines, KYSE-150, TE-1, and normal cell HEEC were obtained from the Shanghai Cell Bank (Shanghai, China). HEEC was cultured in minimum Eagle's medium (Solarbio, Beijing, China). KYSE-150 and TE-1 were grown in (Roswell Park Memorial Institute 1640) RPMI1640 (Gibco, CA, USA) containing 10% fetal bovine serum (FBS) and 1% penicillin-streptomycin at 37 °C in a humidified atmosphere incubator with 5% CO_2.

The lentiviral vectors for knockdown (sh-RBBP7) and the corresponding negative control vectors (sh-NC) were purchased from Shanghai GeneChem company. The sequences of the RBBP7-shRNAs are provided in Table 1. Furthermore, shRNA lentiviral vectors were transfected into ESCC cells using infection enhancer HitransGA

Table 1 Primer Sequences for Genes Used in Transfection and RT-qPCR Assay

Gene	Sequence
GAPDH	Forward: 5′-AGAAGGCTGGGGCTCATTTG-3′
	Reverse: 5′-AGGGGCCATCCACAGTCTTC-3′
shRBBP7-1	Forward: 5′-GTCATCAATGAAGAATATAAAAT-3′
	Reverse: 5′-ATTTTATATTCTTCATTGATGAC-3′
shRBBP7-2	Forward: 5′-AAGAAGAATACACCGTTTCTATA-3′
	Reverse: 5′-TATAGAAACGGTGTATTCTTCTT-3′
RBBP7	Forward: 5′-GAGGAGCGTGTCATCAATGA-3′
	Reverse: 5′-GCATGGGTCATAACCAGGTCA-3′

A (Genechem). Stable infected cells were selected using a medium comprising 1000 ng/mL puromycin for 7 days and Knockdown efficiency was detected by Western blotting.

Cellular irradiation was performed using a medical linear accelerator (Elekta Precise™, Stockholm, Sweden) with 6 MV X-rays. A source-to-surface distance (SSD) of 100 cm was maintained. Cells received single fractions of 2, 4, 6, or 8 Gy at a dose rate of 2 Gy/min. Dosimetric consistency was verified using an ionization chamber prior to experiments.

Quantitative Real-Time Polymerase Chain Reaction (RT-qPCR)

Human ESCC cell lines, KYSE-150, TE-1, and HEEC were in the exponential growth phase. Total RNA was extracted from fresh cells using Trizol reagent (Thermo Scientific, USA). Moreover, cDNA was synthesized using PrimeScript™ (Takara Bio, Japan). Additionally, qRT-PCR was conducted using the SYBR Green PCR kit (Biosharp, Hefei, China) and Roche cobas z480 PCR analyzer (Roche) for synthesized cDNA detection. GAPDH was used as the housekeeping gene. Data were analyzed using the $2^{-(\Delta\Delta Ct)}$ method. The primer sequences for genes are displayed in Table 1.

Western Blotting Analysis

Proteins extracted from cells were subjected to sodium dodecyl sulfate-polyacrylamide gel electrophoresis (SDS-PAGE). Separated proteins were electrophoretically transferred to polyvinylidene difluoride membranes (Merck Millipore, Darmstadt, Germany). The membranes were incubated with primary antibodies RBBP7 (1:1000, ab259957, Abcam, Cambridge, UK), STAT3 (1:2000, ab68153, Abcam), p-STAT3 (1:2000, ab76315, Abcam), Bax (1:4000, 60267-1-Ig, Proteintech, wuhan, China), γ-H2AX (1:2000, ab11174, Abcam), CDK4 (1:2000, ab108357, Abcam), cyclin D1 (1:10000, ab134175, Abcam), Bcl-2 (1:4000, 26593-1-AP, Proteintech), and GADPH (1:1000, 60004-1-Ig, Proteintech) at 4 °C overnight. The proteins were incubated with corresponding secondary antibodies (ab205718, Abcam; S0002, affinity). The protein bands were tested by enhanced chemiluminescence. The densitometric plots of the results were normalized to the intensity of the GAPDH band.

Cell Counting Kit-8 (CCK-8) Assay

Cell viability was determined using a CCK-8 assay (Solarbio, Beijing, China). ESCC cells were inoculated on 96-well plates with 1×10^4 cells per well. Then, an 8 Gy X-ray irradiator was performed after cell adhesion. At 24, 48, and 72 h after IR, 10 μL CCK-8 reagent was added, and cells were incubated at 37 °C for 3 h. The absorbance (OD) value of each pore was measured at 450 nm wavelength on a microplate reader to assess cell viability.

Colony Formation Assay

A colony formation assay was performed using the method proposed by Yu et al.[19] Cells were seeded in six-well plates based on different IR doses and incubated at 37 °C for 24 h. After X-ray radiation, the cells were cultured for two weeks until colonies formed, fixed with 4% paraformaldehyde, and stained with 0.1% crystal violet dye. Colony formation was observed by an inverted phase contrast microscope. GraphPad Prism 6.0 software was used to fit the cell survival curve

with a multi-target single-hit model (Y=1-(1-exp(-k*x))^N), the values of k and N are obtained. Then, based on the formulas: K = 1/D0, lnN = Dq/D_o, the mean lethal dose (D0), quasi-threshold dose (Dq), and radiosensitization ratio (SER= D0(control group)/D0(experimental group)) are calculated for the cells.

Flow Cytometry Analysis

The cells were seeded onto 6 cm plates at 2×10^5 cells/well and incubated at 37 °C for 24 h. The cells were exposed to 8 Gy X-rays. Annexin V-FITC and propyl iodide (PI) staining were performed with an Apoptosis Detection Kit (Solarbio, Beijing, China) for 5 min in dark. Cell cycle: Fixed cells (70% ethanol, −4°C overnight) were treated with RNase A (100 μg/mL, (Solarbio, Beijing, China)) and PI (50 μg/mL) for 30 min. Apoptosis and cell cycle were detected by flow cytometry using CytoFLEX (Beckman Coulter, Suzhou, China) with 488 nm excitation. Apoptotic cells (Annexin V^+ / PI^- early; Annexin V^+ / PI^+ late) and cell cycle phases (FlowJo 10.8.1) were quantified.

Immunohistochemistry (IHC)

The expressions of RBBP7 in ESCC were detected by IHC. First, the paraffin sections of ESCC tissue were dewaxed in xylene. Next, slides were rehydrated in gradient concentrations of ethanol. Then, sections underwent an antigen retrieval process. To inhibit the activity of endogenous peroxidase, 3% H_2O_2 was used. After rinsing in phosphate buffer saline (PBS), 5% goat serum was used to block nonspecific binding sites. Sections were incubated at 4 °C overnight with primary antibodies against RBBP7 (ab259957, Abcam) and incubated with a peroxidase-conjugated secondary antibody (ab205718, Abcam) in the dark. The color was developed using a 3,3'-diaminobenzidine kit (Solarbio, Beijing, China). The specimens were counterstained with hematoxylin before being dehydrated. The staining intensity was graded as <1 (weak staining), 2 (moderate staining), and 3 (strong staining). The percentage of positive cells was graded as 0 (< 5%), 1 (5% ~ < 25%), 2 (25% ~ < 50%), 3 (50% ~ < 75%), and 4 (≥75%). The IHC score was calculated by multiplying staining intensity and the percentage of positive cells relative to the total cells. The results were semi-quantitatively analyzed. Specimens with IHC scores ≥4 were designated positive. The IHC results of RBBP7 were judged by two experienced pathologists who were blinded to clinical and follow-up information.

Immunofluorescence Staining

Immunodetection was conducted as previously described[20] with some modifications. After the slides containing the cells were processed according to the experimental procedures, the slides incubated with RBBP7 (ab259957), γ-H2AX (ab11174) overnight at 4°C, and incubated with the secondary antibody (red) (1:500, ab150080; 1:500, ab150116, abcam). Sections were washed three times, with DAPI staining. Afterwards, slides were mounted in visualized in a laser confocal microscope (DMi8, Germany).

Reactive Oxygen Species (ROS) Assay

The ROS assay kit (Solarbio, Beijing, China) was used according to the manufacturer's instructions, and DCFH-DA was diluted in serum-free medium at 1:15000. Cells were collected and suspended in diluted DCFH-DA and incubated in a cell incubator at 37 °C for 20 minutes. The mixture was reversed every 3 to 5 minutes so that the probe was in full contact with the cell. Cells were washed three times with serum-free cell culture medium to adequately remove DCFH-DA that did not enter the cells. Then ROS were detected by flow cytometry using CytoFLEX.

Clinical Samples

The study included 172 ESCC patients who received radiotherapy with or without concomitant chemotherapy at the Wanbei Coal-Electricity Group General Hospital between January 2020 and October 2023. The surgically resected tissue samples of these patients were fixed with formalin and embedded in paraffin.

The inclusion criteria were as follows: (1) patients with ESCC confirmed by gastroscopy before treatment; (2) Karnofsky score ≥ 70 before radiotherapy; (3) no esophageal fistula formation; (4) baseline examinations such as chest (computed tomography) CT, abdominal, and supraclavicular color ultrasound were performed before radiotherapy; (5) no history of distant metastasis or other malignant tumors; (6) no serious respiratory, circulatory, or endocrine diseases. In

addition, we collected clinical data from these patients, including gender, tumor characteristics, tumor-lymph node metastasis (TNM) stage (according to the 8th edition of the AJCC TNM staging guidelines), etc. The specific clinical data are shown in Table 2.

The use of tissue specimens and clinical information was approved by the Ethics Committee of the Wanbei Coal-Electricity Group General Hospital, The study was conducted in accordance with the Declaration of Helsinki, and all methods were implemented following relevant guidelines and regulations.

Statistical Analysis

All statistical analyses were performed using SPSS 21.0 and GraphPad Prism 6.0. In addition, the χ^2 test was used for categorical variables. The Student's *t*-test (for normally distributed data) was applied for comparisons between two groups or Mann–Whitney *U*-test (for non-normal data), analysis of variance (ANOVA) was employed for comparisons among multiple groups, and Tukey's post-hoc test was used for pairwise comparisons following ANOVA. $P < 0.05$ was considered statistically significant.

Table 2 Clinical Characteristics of ESCC Patients

Characteristics	Category	No. (%)
Gender	Male	125 (72.67)
	Female	47 (27.33)
Age, median, range		71 (44–87)
Tumor site	Cervical segment	7 (4)
	Upper thoracic portion	31 (18.02)
	Middle thoracic portion	95 (55.23)
	Low thoracic portion	39 (22.67)
Differentiation	Highly differentiation	36 (20.93)
	Medium differentiation	99 (57.56)
	Low differentiation	37 (21.51)
Myelosuppression	No	63 (36.63)
	Yes	109 (63.37)
Whether combined with chemotherapy	No	120 (69.77)
	Yes	52 (30.23)
Radiotherapy	3D conformal	57 (33.14)
	Intensity modulation	115 (66.86)
TNM-staging	II stage	130 (75.58)
	III - IVstage	42 (24.42)
Lymph node metastasis	No	133 (77.33)
	Yes	39 (22.67)

Note: Concurrent chemoradiotherapy (chemotherapy regimen was platinum-based combined chemotherapy or tegafur, gimeracil, and oteracil potassium capsules single-agent chemotherapy).
Abbreviation: TNM, tumor-node-metastasis.

https://doi.org/10.2147/OTT.S535750

Results

Expression of RBBP7 in ESCC

We analyzed the (tumor immune estimation resource) TIMER database (https://cistrome.shinyapps.io/timer/) and found that RBBP7 is highly expressed in various cancers, including breast cancer, cholangiocarcinoma, colon cancer, esophageal cancer, head and neck tumor and lung cancer ($P < 0.01$, Figure 1A and B), with statistical significance of gene differential expression evaluated using the Wilcoxon test. According to (the University of Alabama at Birmingham cancer data analysis portal) UALCAN database analysis (https://ualcan.path.uab.edu/analysis.html), the RBBP7 gene is associated with individual cancer stages, cancer grade (2 and 3), and nodal metastasis status ($P < 0.05$, Figure 1C–E). We performed the Gene Expression Profiling Interactive Analysis (GEPIA) database (http://gepia.cancer-pku.cn/) analysis and found that RBBP7 is associated with a poor outcome in ESCC patients ($P < 0.01$, Figure 1F and G).

RBBP7 expression in ESCC tissues and adjacent normal tissues was detected by RT-qPCR, which showed that RBBP7 expression was increased in ESCC tissues ($P < 0.01$, Figure 1H). RBBP7 expression in ESCC cells was determined using RT-qPCR and Western blot, which suggested that compared with HEEC, mRNA and protein levels of RBBP7 were highly expressed in ESCC cells ($P < 0.05$, Figure 1I and J). To investigate the localization of RBBP7 on ESCC cells, we performed immunofluorescence and found that RBBP7 was predominantly located in the cell nuclei in the TE-1 and KYSE-150 ESCC cell lines (Figure 1K). Western blotting was performed to detect transfection efficiency after inhibiting RBBP7 on ESCC cells, the results revealed reduced protein expressions of sh-RBBP7-1 and sh-RBBP7-2 ($P < 0.05$). Furthermore, shRBBP7-2, with the best interference effect, was selected for subsequent studies (Figure 1L and M).

Knockdown of RBBP7 Could Bidirectional Modulation of Cell Proliferation and Radiosensitivity

Subsequent functional experiments, the CCK-8 results revealed that RBBP7 knockdown significantly modulated radiation-induced cell death in a cell type-dependent manner. In TE-1 cells, shRBBP7 combined with IR reduced cell viability compared to IR alone ($P < 0.01$). Conversely, in KYSE-150 cells, shRBBP7 + IR increased cell viability relative to the IR group ($P < 0.01$) (Figure 2A and B). Further experiments demonstrated that RBBP7 knockdown suppressed proliferation in TE-1 cells but enhanced proliferation in KYSE-150 cells.

Clonogenic assays were performed to evaluate the long-term proliferative capacity and radiosensitivity of control (sh-NC) and RBBP7 knockdown cells across KYSE-150 and TE-1 lines following 6 MV X-rays (0, 2, 4, 6, and 8 Gy). After 10–14 days of culture, colony formation rates were quantified (Figure 2C and E). In TE-1 cells, survival fractions (SF) decreased with increasing radiation doses (Figure 2D), with shRBBP7 significantly reducing survival at 2 Gy compared to sh-NC controls (0.325 versus 0.434; $P < 0.05$, Figure 2G). KYSE-150 cells exhibited increased SF with increasing radiation doses (Figure 2F). where shRBBP7 demonstrated higher survival at 2 Gy compared to sh-NC controls (0.318 versus 0.291; $P > 0.05$, Figure 2G). Moreover, The radiosensitization ratio (SER) values for TE-1 and KYSE-150 cells were $1.370 > 1$ and $0.771 < 1$, respectively, indicating that shRBBP7 can enhance the radiosensitivity of TE-1 cells, whereas it reduces the radiosensitivity of KYSE-150 cells.

Since ionizing radiation is known to generate ROS in cellular systems, we quantitatively assessed intracellular ROS levels in ESCC cell lines following different treatment conditions. Our results demonstrated cell line-specific responses to RBBP7 knockdown under irradiation (Figure 2H and I). In TE-1 cells, both IR and sh-RBBP7 groups showed significantly elevated ROS levels compared to NC group ($P < 0.01$). The sh-RBBP7 + IR (8Gy) exhibited synergistic ROS induction, with levels markedly exceeding irradiation alone ($P < 0.01$). In KYSE-150 cells, RBBP7 knockdown alone significantly reduced basal ROS ($P < 0.05$ versus NC). Contrary to TE-1 cells, the combination treatment showed attenuated ROS generation compared to IR-only controls. These differential responses suggest that RBBP7 depletion mediates radiosensitivity through ROS-dependent mechanisms in a cell context-specific manner: promoting oxidative stress in TE-1 cells (enhancing radiation efficacy) while exhibiting antioxidant effects in KYSE-150 cells (contributing to radioresistance).

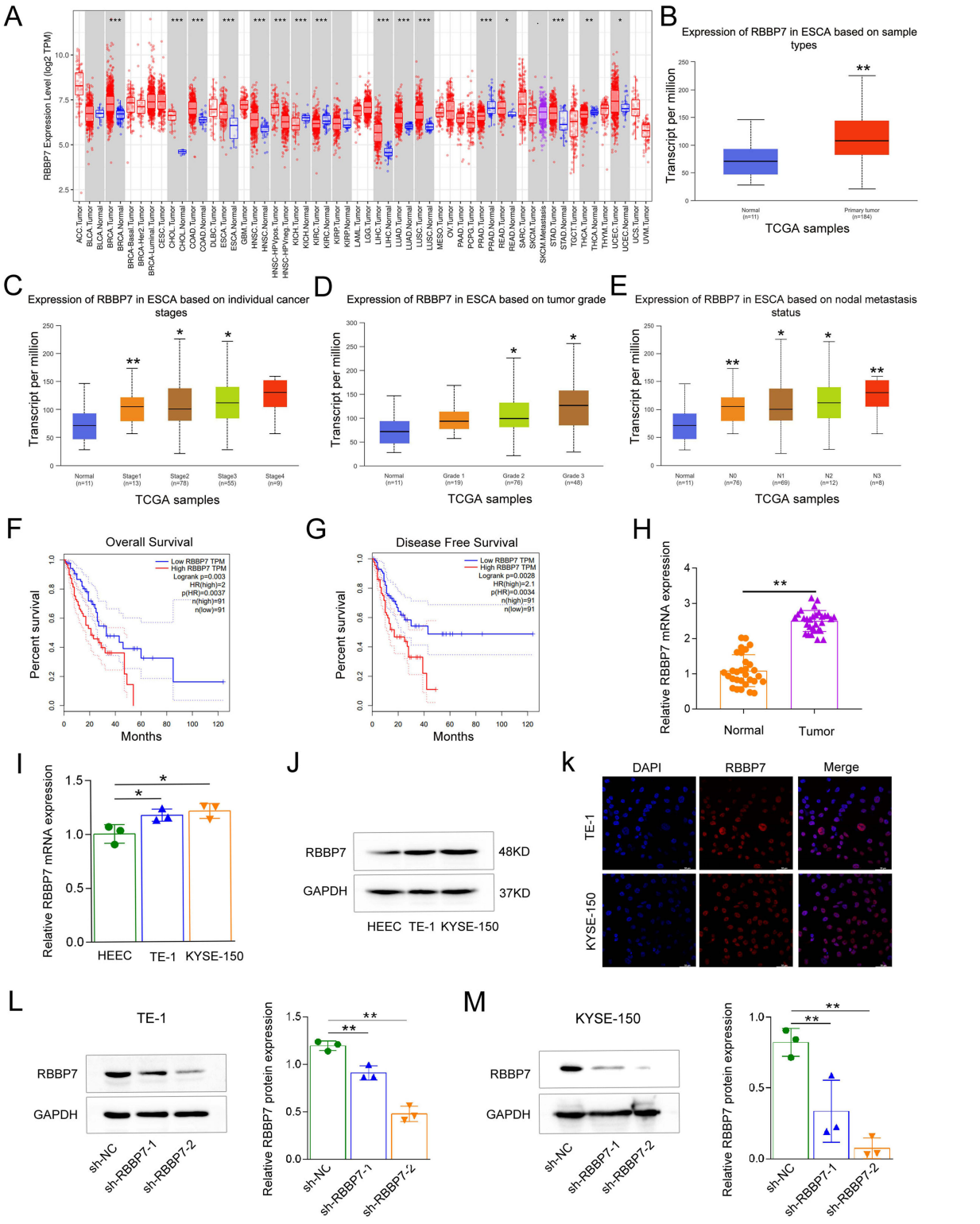

Figure 1 RBBP7 is aberrantly expressed in various human carcinomas and ESCC. (**A**) The expression of RBBP7 in multiple cancer species and the difference between RBBP7 and normal tissue were analyzed using the TIMER database; (**B–E**) RBBP7 expression in Esophageal carcinoma (ESCA) based on sample types, cancer stage grade, and nodal metastasis status was analyzed by the UALCAN database (*P < 0.05, **P < 0.01, ***P < 0.001). (**F** and **G**) RBBP7-related overall survival (OS) and disease-free survival (DFS) curves in ESCC patients were analyzed by the GEPIA database. (**H**) RBBP7 expression in ESCC tissues and adjacent normal tissues was detected by RT-qPCR (n = 30), **P < 0.01 versus the normal group; (**I** and **J**) RBBP7 expressions in TE-1 and KYSE-150 cells were detected by RT-qPCR and Western blotting assay, ** P < 0.01, * P < 0.05 versus the HEEC group. (**K**) the location of RBBP7 in ESCC cells was tested by Immunofluorescence assay (magnification, x100). (**L** and **M**) RBBP7 expressions after knockdown detected by Western blotting assay, ** P < 0.01, * P < 0.05 versus the sh-NC group.

https://doi.org/10.2147/OTT.S535750

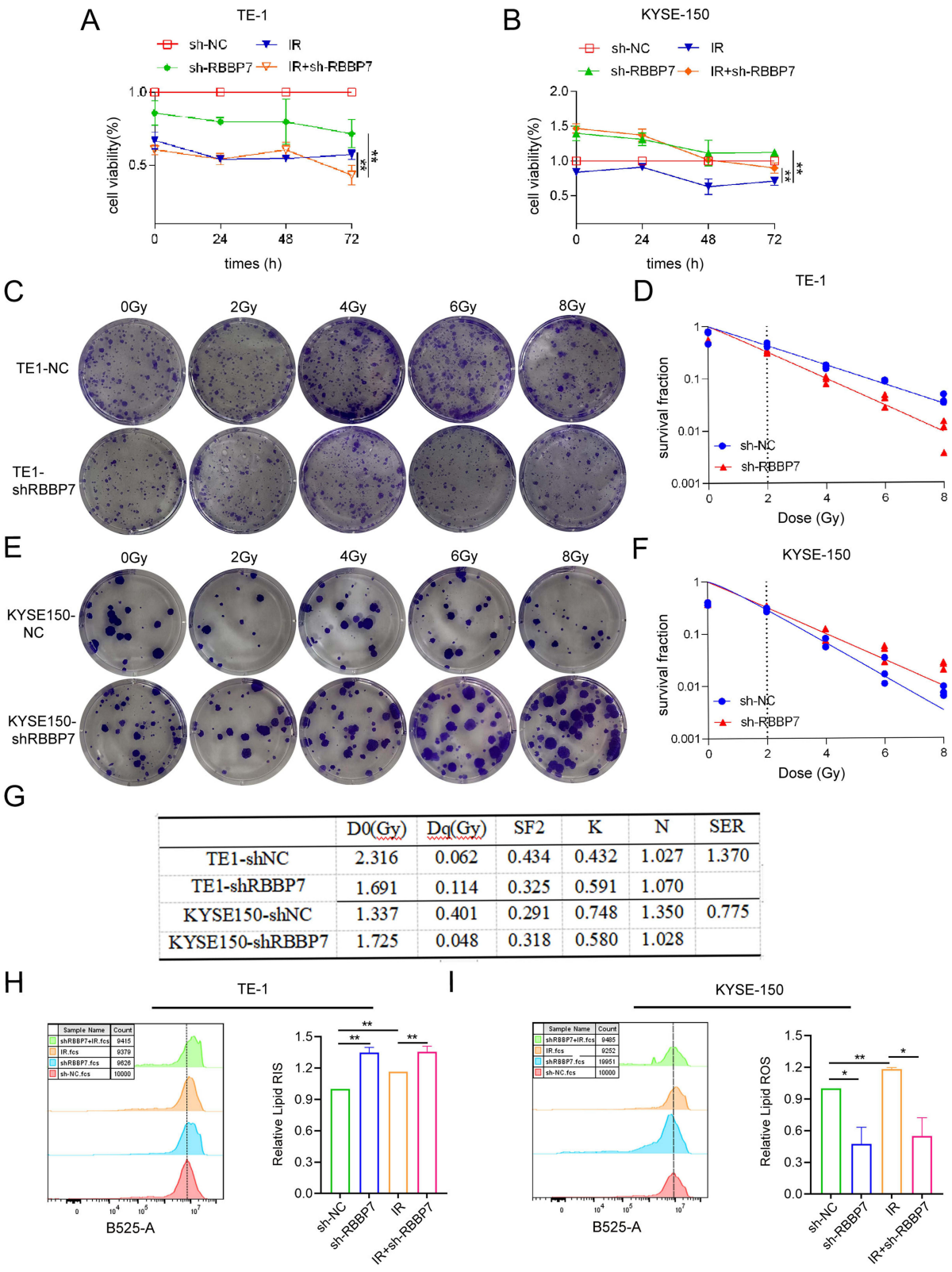

	D0(Gy)	Dq(Gy)	SF2	K	N	SER
TE1-shNC	2.316	0.062	0.434	0.432	1.027	1.370
TE1-shRBBP7	1.691	0.114	0.325	0.591	1.070	
KYSE150-shNC	1.337	0.401	0.291	0.748	1.350	0.775
KYSE150-shRBBP7	1.725	0.048	0.318	0.580	1.028	

Figure 2 RBBP7 expression in ESCC cells and its different effects on the proliferation and radiosensitivity of ESCC cells. (**A** and **B**) CCK-8 assay was used to detect the proliferation activity of TE-1 and KYSE-150 cells at 24, 48 and 72 h after 8 Gy X-ray irradiation. (**C** and **E**) Cells were irradiated with 0, 2, 4, 6, and 8 Gy X-rays and cultured for 10–14 days, the colony formation ability of KYSE-150 and TE-1 cells after RBBP7 silencing was observed by colony formation assay. (**D** and **F**) The survival curves of TE-1 and KYSE-150 cells following RBBP7 gene silencing fitted by a multi-target single-hit model. (**G**) The radiobiology parameters in 2 Gy of TE-1 and KYSE-150 cells following RBBP7 knockdown calculated by a multi-target single-hit model, D0: mean lethal dose; Dq: quasi-threshold dose; N: extrapolation number; SF: Survival fraction; SER: survival enhancement ratio, SER= D0(control)/D0(experimental). (**H** and **I**). Detection of ROS levels by flow cytometry analysis in TE-1 and KYSE-150 cells. ** $P < 0.01$, * $P < 0.05$. IR: irradiation.

Knockdown of RBBP7 Could Regulate Cell Cycle and Apoptosis Differently

To further investigate the impact of RBBP7 on cell cycle regulation following X-ray irradiation, we performed flow cytometry analysis on ESCC cells exposed to 8 Gy radiation. The results revealed distinct cell cycle arrest patterns. RBBP7 knockdown alone causes TE-1 cells to arrest in the S phase of the cell cycle, while KYSE-150 cells arrest in the G0/G1 phase. Notably, RBBP7 knockdown combined with IR leads to an arrest in the G2/M phase for both TE-1 and KYSE-150 cells, with the arrest being less pronounced in KYSE-150 cells (73.45±2.98)% compared to TE-1 cells (86.95 ±0.45)% (Figure 3A). CDK4 and Cyclin D1 are important cell cycle-related proteins. Western blot analysis of protein expression levels showed that compared with the IR group, the protein expression levels of both Cyclin D1 and CDK4 in TE-1 cells treated with RBBP7 knockdown combined with IR were significantly downregulated ($P < 0.01$). In KYSE-150 cells, The same treatment paradoxically upregulated CDK4 ($P < 0.05$) while downregulating Cyclin D1 ($P < 0.01$) (Figure 3B). These findings suggest that RBBP7 modulates radiation-induced cell cycle arrest through differential regulation of cyclin-CDK complexes in a cell line-dependent manner, potentially contributing to the observed differences in radiosensitivity.

γ-H2AX, a phosphorylated histone H2AX variant, serves as both a critical DNA damage response factor and a sensitive biomarker of DNA double-strand breaks (DSBs). Quantitative monitoring of γ-H2AX provides essential insights into radiation-induced DNA damage and cellular repair capacity during radiotherapy evaluation. Our analysis revealed cell line-specific γ-H2AX expression patterns following combinatorial treatment (Figure 3C and D). In TE-1 cells, RBBP7 knockdown combined with IR (8 Gy) significantly increased γ-H2AX levels versus irradiation alone ($P < 0.01$). These differential responses suggest that RBBP7 knockdown compromises DNA DSBs repair fidelity in TE-1 cells, leading to persistent DNA damage. Conversely, In KYSE-150 cells, The same treatment reduced γ-H2AX expression compared to IR-only controls, although statistically non-significant, the downward trend in γ-H2AX suggests reduced DNA damage signaling in this poorly differentiated cell line, aligning with its radioresistant phenotype.

Flow cytometry for detecting cell apoptosis exposed that in TE-1 cells, the apoptosis rate in the IR + sh-RBBP7 group was significantly increased than both IR alone (12.66% ±0.52% versus 9.25% ± 0.75%; $P < 0.01$) and sh-RBBP7 alone (12.66% ±0.52% versus 8.95% ± 0.87%; $P < 0.01$). Conversely, KYSE-150 cells showed reduced apoptosis in the IR + sh-RBBP7 group relative to IR alone (6.32% ± 0.51% versus 9.11% ± 0.20%; $P < 0.01$) and sh-RBBP7 alone (6.32% ± 0.51% versus 7.72% ± 0.26%; $P < 0.05$), indicating that RBBP7 knockdown could promote radiation-induced apoptosis in TE-1 cells while exerting anti-apoptotic effects in KYSE-150 cells (Figure 3E and F).

RBBP7 Knockdown Differentially Modulates STAT3 Phosphorylation in ESCC Cell Lines

To investigate the mechanistic basis of RBBP7-mediated radiosensitivity, we examined its relationship with STAT3 signaling The GEPIA database revealed a significant positive correlation between RBBP7 and STAT3 expression in ESCC ($R = 0.11$, $P < 0.01$) (Figure 4A). Subsequent Western blot analysis demonstrated cell type-specific modulation of STAT3 phosphorylation, in TE-1 cells, RBBP7 knockdown combined with IR synergistically suppressed p-STAT3 levels (0.38-fold reduction versus NC alone, $P < 0.01$) and p-STAT3/STAT3 ratio (1.07-fold reduction versus IR alone, $P > 0.05$). Whereas KYSE-150 cells exhibited paradoxical p-STAT3 hyperactivation (1.76-fold increase versus NC alone, $P < 0.01$) and p-STAT3/STAT3 ratio (2.05-fold increase versus IR alone, $P < 0.01$) under identical treatment conditions (Figure 4B and C).

RBBP7 Expression and Its Correlation with Clinicopathological Parameters in ESCC

IHC analysis revealed RBBP7 was predominant nuclear localization of RBBP7 in ESCC specimens (Figure 4D). Among 172 evaluable cases, RBBP7 positivity was observed in 51.7% (89/172) of tumors, with the remaining 48.3% (83/172) classified as negative. This overexpression pattern was significantly associated with key clinicopathological parameters (Table 3). Highly differentiated tumors showed lower RBBP7 positivity (33.3%, 12/36) compared to moderately (54.5%, 54/99) and poorly differentiated tumors (59.5%, 22/37). The proportion of RBBP7-positive cases increased with

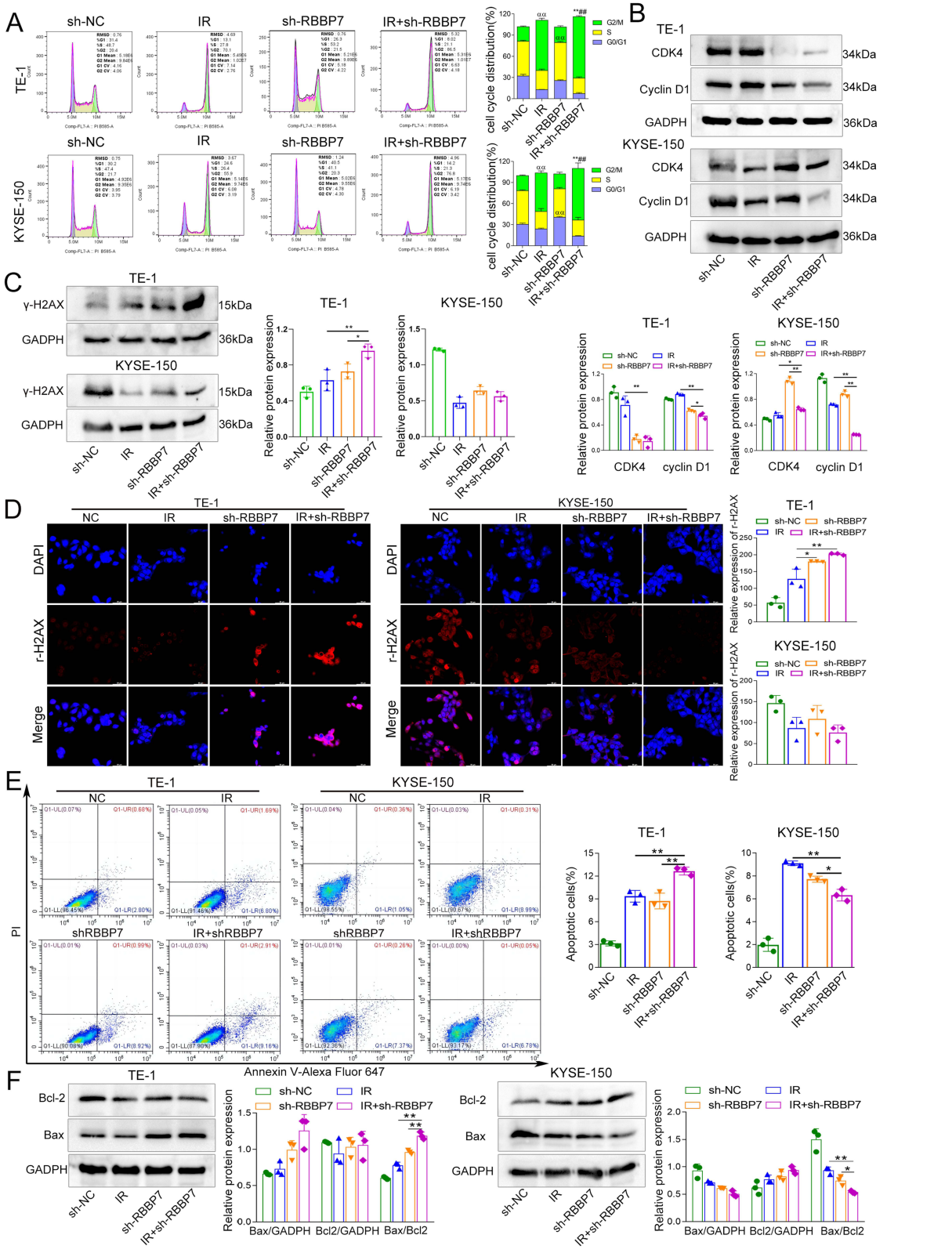

Figure 3 The cycle and apoptosis of ESCC cells were detected after 8Gy X-ray irradiation. (**A**) Cell cycle assay results and analysis figures, $^{\alpha\alpha}P < 0.01$ versus the sh-NC group; $^{**}P < 0.01$ versus the sh-RBBP7 group; $^{\#\#}P < 0.01$ versus the IR group. (**B**) shRBBP7 regulated cell cycle protein expression. (**C**) Western blot analysis of γ-H2AX protein expression in ESCC cell after IR and shRBBP7 treatment. GAPDH served as a loading control. (**D**) Representative immunofluorescence images showing γ-H2AX foci formation under the same conditions (magnification, x100). (**E** and **F**) Cells apoptosis assay results and apoptosis-related proteins were detected. $^{**}P < 0.01$, $^{*}P < 0.05$. IR: X-ray irradiation.

https://doi.org/10.2147/OTT.S535750

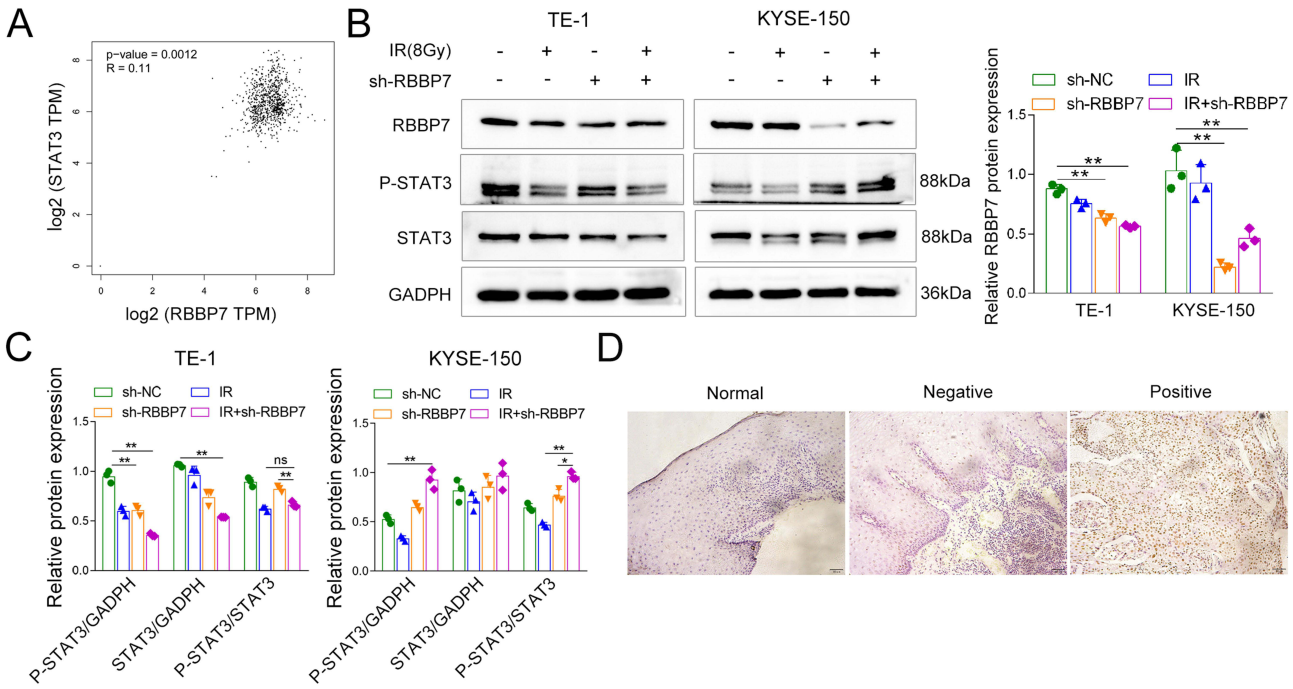

Figure 4 RBBP7 Knockdown Differentially Modulates STAT3 Phosphorylation in ESCC Cell Lines. (**A**) Correlation of RBBP7 and STAT3 expressions analyzed using the GEPIA database (R = 0.11, $P < 0.01$). (**B** and **C**) Representative Western blotting of RBBP7, STAT3, p-STAT3 (Tyr705) levels in TE-1 and KYSE-150 cells with or without IR and downregulation of RBBP7. GAPDH was used as a loading control, Band intensities were quantified by ImageJ and normalized to GAPDH or STAT3 (for phosphorylation ratio). (**D**) Representative images of normal, negative, and positive RBBP7 staining in ESCC tumor tissues (magnification, x200). $^{**}P < 0.01$, $^{*}P < 0.05$. IR: X-ray irradiation.

decreasing differentiation grade (χ^2=6.05). Advanced stage (III–IV) tumors exhibited significantly higher RBBP7 positivity (64.3%, 27/42) versus early stage (II) tumors (45.4%, 59/130). The 1.4-fold increase in RBBP7 positivity in advanced stages indicates its potential as a progression marker. In addition, the nuclear predominance of RBBP7 suggests its potential role in transcriptional regulation or chromatin remodeling during ESCC progression.

Table 3 Relationship Between RBBP7 Expression and Clinicopathological Features of Patients with ESCC

Variables	Total (n=172)	RBBP7 Level		χ^2	*P-value*
		Negative	Positive		
Gender				1.59	0.208
Male	125	64	61		
Female	47	19	28		
Age				1.75	0.186
<65 year	43	17	26		
≥65 year	129	66	63		
Tumor site				2.17	0.537
Cervical segment	7	5	2		
Upper thoracic portion	31	13	18		
Middle thoracic portion	95	45	50		
Low thoracic portion	39	20	19		
Differentiation				6.05	0.048*
Highly differentiation	36	24	12		
Medium differentiation	99	45	54		
Low differentiation	37	14	23		

(*Continued*)

https://doi.org/10.2147/OTT.S535750

Table 3 (Continued).

Variables	Total (n=172)	RBBP7 Level		χ^2	*P-value*
		Negative	Positive		
Myelosuppression				0.04	0.850
No	63	31	32		
Yes	109	52	57		
Whether combined with chemotherapy				2.86	0.091
No	120	63	57		
Yes	52	20	32		
Radiotherapy				4.43	0.035*
3D conformal	57	34	23		
Intensity modulation	115	49	66		
TNM-staging				4.54	0.033*
II stage	130	70	60		
III-IV stage	42	13	29		
Lymph node metastasis				0.44	0.507
No	133	66	67		
Yes	39	17	22		

Note: *$P < 0.05$.
Abbreviation: TNM, tumor-node-metastasis.

Discussion

Despite declining incidence rates of esophageal squamous cell carcinoma (ESCC) in China, mortality remains persistently high due to intrinsic radioresistance and limited therapeutic options.[21] Radiotherapy, a cornerstone of multimodal ESCC treatment, often fails to achieve durable local control, with 5-year survival rates remaining below 20% for advanced-stage disease. Improving radiosensitivity represents an urgent clinical imperative to enhance therapeutic efficacy and prolong patient survival. This study explores RBBP7—a chromatin remodeling factor involved in DNA damage response and cell cycle control—as a candidate molecular regulator of radiation response.

RBBP7 functions as a multifaceted epigenetic regulator with documented roles in tumor proliferation, apoptosis, and cell cycle progression across malignancies. Its functionality exhibits context-dependent duality, demonstrating both tumor-promoting and tumor-suppressive activities in distinct cancer types. However, its context-dependent functionality remains incompletely resolved. This functional dichotomy—potentially dictated by tissue-specific interactors (eg, transcription factors) and cellular microenvironment. Critically, prior ESCC studies focused solely on its role in untreated cells,[10] overlooking its unexplored function in radiation reponse.

In this study, Bioinformatic analysis revealed elevated RBBP7 expression across multiple malignancies, including esophageal carcinoma, with high expression levels significantly correlating with poor survival prognosis in ESCC patients. To investigate the functional link between RBBP7 and radiobiological responses in ESCC, we employed two cell lines with distinct differentiation statuses: well-differentiated TE-1 and poorly-differentiated KYSE-150. Notably, RBBP7 exhibited dichotomous regulation of radiosensitivity in a cell line-dependent manner. In well-differentiated TE-1 cells, RBBP7 knockdown synergized with IR to amplify ROS generation (1.2-fold versus IR alone; $P<0.01$); impair DNA DSB repair, evidenced by elevated γ-H2AX expression (shRBBP7 + IR group versus IR-alone; $P<0.05$), thereby apoptosis increased; and induce G2/M arrest (86.95% versus 73.45% in KYSE-150) through coordinated downregulation of Cyclin D1 and CDK4, thereby inhibiting cell proliferation. These effects collectively enhanced radiosensitivity (SER=1.37). Conversely, in poorly differentiated KYSE-150 cells, RBBP7 knockdown synergized with IR to reduced ROS production (0.5-fold versus IR; $P<0.05$), non-significant reduction in γ-H2AX (versus IR; $P>0.05$) and apoptosis decreased, suggesting preserved DNA repair fidelity, Specifically, RBBP7 silencing may activate compensatory alternative DSB repair pathways in aggressive ESCC subtypes, enabling sustained proliferation. Moreover, Paradoxical CDK4 upregulation (versus IR; $P<0.05$) despite Cyclin D1 suppression ($P<0.01$). Multiple studies have demonstrated

that the CDK-RB-E2F pathway is critical for the control of cell proliferation.[22] CDK4 upregulation coupled with Cyclin D1 suppression may suggest an adaptive feedback mechanism: by activating alternative cell cycle drivers (eg, E2F-CDK4 axis), tumor cells bypass G1/S checkpoint activation, sustain proliferative capacity,[23] and ultimately develop radioresistance. These effects collectively enhanced radioresistance (SER=0.775).

STAT3, a transcription factor that regulates the expression of various genes related to biological processes such as cell proliferation, cell cycle control, inhibition of apoptosis, and immune modulation,[24–26] It is established that STAT3 signaling contributes to radioresistance in colorectal and prostate cancers,[27–29] and pharmacological STAT3 inhibition can enhance radiosensitivity to improve therapeutic outcomes.[28,29] Given this conserved role across malignancies, Moreover, serves as a pivotal downstream effector of RBBP7 signaling,[30] we sought to preliminarily determine whether STAT3/p-STAT3 activation would be affected after combined RBBP7-IR intervention. Bioinformatic analysis revealed a positive correlation between RBBP7 and STAT3 expression (R=0.11, $P<0.01$). Functional validation demonstrated cell type-specific modulation, in well-differentiated TE-1 cells, RBBP7 knockdown combined with IR suppressed p-STAT3 activation (decrease in p-STAT3/STAT3 ratio), triggering a pro-apoptotic shift (increased Bax/Bcl-2 ratio). In poorly differentiated KYSE-150 cells, RBBP7-independent p-STAT3 hyperactivation occurred post-IR, sustaining anti-apoptotic programs (decreased Bax/Bcl-2 ratio), This aligns with established oncogenic functions of STAT3 in esophageal cancer, where elevated STAT3 phosphorylation enhances proliferative capacity.[31] In addition, STAT3 activation transcriptionally upregulates cyclin D1 to drive CDK4/6-mediated Rb phosphorylation and G1/S progression.[32,33] Other studies have shown that STAT3 can also promote or inhibit proliferation depending on upstream signals and the specific cellular context.[34,35] Given that the RBBP7-HDAC1 complex catalyzes histone deacetylation at STAT3 target genes (eg, the Cyclin D1 promoter) to repress their transcription,[30] we hypothesize that RBBP7 dictates radiosensitivity by spatiotemporally modulating the STAT3-CyclinD1/CDK4 pathway, thereby inducing differentiation-dependent cell cycle arrest patterns in cancer cells. In well-differentiated TE-1 cells: RBBP7 silencing derepresses the STAT3-CyclinD1 axis, activating the G1/S checkpoint and arresting cells at the DNA repair-deficient G2/M phase, consequently enhancing radiosensitivity. However, in poorly differentiated KYSE-150 cells: RBBP7 knockdown activates p-STAT3, leading to paradoxical CDK4 upregulation that drives checkpoint escape, sustains proliferation, and confers radioresistance. Notably, the mechanisms by which RBBP7-STAT3 signaling mediates compensatory CDK4 upregulation and Cyclin D1 suppression in KYSE-150 cells, along with the precise regulation of STAT3 activity by RBBP7 across differentially differentiated cellular contexts, remain unresolved. Furthermore, direct causal links between the RBBP7-STAT3 axis and radiosensitivity await future validation. Although these mechanistic gaps persist, they do not compromise the core conclusions of this study and will be further explored in the future.

Due to the opposite results observed in the two cell lines in this experiment, studies have shown that poorly differentiated cells have higher proliferative and invasive capabilities,[36] and may have stronger radiotherapy resistance,[37] which may be due to differences in DNA damage repair, cell cycle regulation, and apoptotic pathways, this is consistent with our cell cycle and other findings described above. Subsequently, to further determine the expression of RBBP7 in ESCC tissues and its correlation with clinical parameters, we collected pathological tissue specimens and clinical case data from patients with ESCC undergoing radiotherapy. The results showed that highly differentiated tumors showed lower RBBP7 positivity (33.3%) compared to poorly differentiated tumors (59.5%). The proportion of RBBP7-positive cases increased with decreasing differentiation grade, advanced stage (III–IV) tumors exhibited significantly higher RBBP7 positivity. This again indicates that the different roles of RBBP7 in the two cell lines may be related to the different degrees of cell differentiation.

This study has certain limitations. First, the research was primarily conducted using two cell lines, TE-1 and KYSE-150. Although these cell lines provided valuable preliminary data for the study, they cannot fully represent the biological characteristics and diversity of the patient population of all ESCCs. Significant genetic and phenotypic heterogeneity among different ESCC patients may affect the expression patterns of RBBP7 and the response to radiotherapy. Second, using only two cell lines may limit the generalizability and extrapolation capability of the study results. To understand the role of RBBP7 more comprehensively in ESCC, future research should include more cell lines and patient-derived xenograft (PDX) models, which can better simulate the complexity of human tumors. Moreover, while this study

suggested a correlation between RBBP7 and the STAT3/p-STAT3 signaling pathway, the detailed molecular mechanisms of how this pathway specifically regulates the radiotherapy response of ESCC cells still need further clarification.

Conclusion

In summary, we reported the novel phenomenon that RBBP7 exhibits elevated expression in ESCC and correlates with poor patient prognosis. Its upregulation is significantly associated with advanced tumor stage and poor differentiation. Crucially, RBBP7 bidirectionally regulates radiosensitivity in a differentiation-dependent manner: its depletion enhances radiosensitivity in well-differentiated TE-1 cells by inducing G2/M arrest, amplifying ROS, impairing DNA repair (γ-H2AX expression was increased), and promoting apoptosis, yet confers radioresistance in poorly differentiated KYSE-150 cells via CDK4 upregulation, suppressed ROS production, and attenuated apoptosis. Our work reveals that cellular differentiation states dictate functional outputs of the STAT3 pathway, providing a mechanistic basis for context-specific radiotherapy responses in ESCC.

Data Sharing Statement

The original contributions presented in the study are included in the article. Further inquiries can be directed to the corresponding author.

Ethics Statement

This study was approved by the Ethics Committee of the General Hospital of Wanbei Coal-Electricity Group (No.: WBZY-LLWYH-2025-10) and was confirmed as a risk-exempt retrospective study. All pathological tissue paraffin blocks and clinical data were derived from historical archives and have been completely anonymized by removing personal identifiers, ensuring no linkage to specific individuals, this study meets the criteria for exemption from informed consent. Data usage strictly adheres to privacy protection principles and is solely for scientific research purposes.

Author Contributions

All authors made a significant contribution to the work reported, whether that is in the conception, study design, execution, acquisition of data, analysis and interpretation, or in all these areas; took part in drafting, revising or critically reviewing the article; gave final approval of the version to be published; have agreed on the journal to which the article has been submitted; and agree to be accountable for all aspects of the work.

Funding

This work was supported by Suzhou Science and Technology Bureau Foundation (SZWJ2023a055); Natural Science Foundation of Bengbu Medical University(2023byzd260); Scientific research project of Suzhou Health Commission (SZWJ2023a080; SZWJ2023 a076).

Disclosure

The authors declare no conflicts of interest regarding the publication of this paper.

References

1. Bray F, Laversanne M, Sung H, et al. Global cancer statistics 2022: GLOBOCAN estimates of incidence and mortality worldwide for 36 cancers in 185 countries. *CA-Cancer J Clin*. 2024;74:229–263. doi:10.3322/caac.21834
2. Bray F, Ferlay J, Soerjomataram I, et al. Global cancer statistics 2018: GLOBOCAN estimates of incidence and mortality worldwide for 36 cancers in 185 countries. *CA-Cancer J Clin*. 2018;68(6):394–424. doi:10.3322/caac.21492
3. Allemani C, Matsuda T, Di Carlo V, et al. Global surveillance of trends in cancer survival 2000-14 (Concord-3): analysis of individual records for 37 513 025 patients diagnosed with one of 18 cancers from 322 population-based registries in 71 countries. *Lancet*. 2018;391:1023–1075. doi:10.1016/S0140-6736(17)33326-3
4. Cai L, Liu B, Cao Y, Sun T, Li Y. Unveiling the molecular structure and role of RBBP4/7: implications for epigenetic regulation and cancer research. *Front Mol Biosci*. 2023;10:1276612. doi:10.3389/fmolb.2023.1276612
5. Wu H, Moshkina N, Min J, et al. Structural basis for substrate specificity and catalysis of human histone acetyltransferase 1. *Proc Natl Acad Sci USA*. 2012;109:8925–8930. doi:10.1073/pnas.1114117109

6. Li HJ, Yu PN, Huang KY, et al. NKX6.1 functions as a metastatic suppressor through epigenetic regulation of the epithelial-mesenchymal transition. *Oncogene*. 2016;35:2266–2278. doi:10.1038/onc.2015.289
7. Li GC, Guan LS, Wang ZY. Overexpression of RbAp46 facilitates stress-induced apoptosis and suppresses tumorigenicity of neoplastigenic breast epithelial cells. *Int, J, Cancer*. 2003;105:762–768. doi:10.1002/ijc.11148
8. Chen GC, Guan LS, Yu JH, et al. Rb-associated protein 46 (RbAp46) inhibits transcriptional transactivation mediated by BRCA1. *Biochem Biophys Res Commun*. 2001;284:507–514. doi:10.1006/bbrc.2001.5003
9. Yeh HH, Tseng YF, Hsu YC, et al. Ras induces experimental lung metastasis through up-regulation of RbAp46 to suppress RECK promoter activity. *BMC Cancer*. 2015;15:172. doi:10.1186/s12885-015-1155-7
10. Yu N, Zhang P, Wang L, et al. RBBP7 is a prognostic biomarker in patients with esophageal squamous cell carcinoma. *Oncol Lett*. 2018;16:7204–7211. doi:10.3892/ol.2018.9543
11. Zhan Y, Yin A, Su X, et al. Interpreting the molecular mechanisms of RBBP4/7 and their roles in human diseases (Review). *Int J Mol Med*. 2024;53:48. doi:10.3892/ijmm.2024.5372
12. Guan LS, Li GC, Chen CC, et al. Rb-associated protein 46 (RbAp46) suppresses the tumorigenicity of adenovirus-transformed human embryonic kidney 293 cells. *Int, J, Cancer*. 2001;93:333–338. doi:10.1002/ijc.1338
13. Wang R, Huang Z, Lin Z, et al. Hypoxia-induced RBBP7 promotes esophagus cancer progression by inducing CDK4 expression. *Acta Biochim Biophys Sin*. 2022;54:179–186. doi:10.3724/abbs.2021027
14. Guo H, Xiao Y, Yuan Z, et al. Inhibition of $STAT3^{Y705}$ phosphorylation by stattic suppresses proliferation and induces mitochondrial-dependent apoptosis in pancreatic cancer cells. *Cell Death Discov*. 2022;8:116. doi:10.1038/s41420-022-00922-9
15. Dong L, Liu C, Sun H, et al. Targeting STAT3 potentiates CDK4/6 inhibitors therapy in head and neck squamous cell carcinoma. *Cancer Lett*. 2024;593:216956. doi:10.1016/j.canlet.2024.216956
16. Aaronson DS, Horvath CM. A road map for those who don't know JAK-STAT. *Science*. 2002;296:1653–1655. doi:10.1126/science.1071545
17. Wang M, Meng B, Liu Y, et al. MiR-124 inhibits growth and enhances radiation-induced apoptosis in non-small cell lung cancer by inhibiting STAT3. *Cell Physiol Biochem*. 2017;44:2017–2028. doi:10.1159/000485907
18. Zhang Q, Zhang C, He J, et al. STAT3 inhibitor stattic enhances radiosensitivity in esophageal squamous cell carcinoma. *Tumour Biol*. 2015;36:2135–2142. doi:10.1007/s13277-014-2823-y
19. Yu D, Ma Y, Feng C, et al. PBX1 increases the radiosensitivity of oesophageal squamous cancer by targeting of STAT3. *Pathol Oncol Res*. 2020;26:2161–2168. doi:10.1007/s12253-020-00803-5
20. Li L, Zhu G, Tan K, et al. CUX2/KDM5B/SOX17 axis affects the occurrence and development of breast cancer. *Endocrinology*. 2022;163:bqac110. doi:10.1210/endocr/bqac110
21. Shapiro J, van Lanschot JJB, Hulshof MCCM, et al. Neoadjuvant chemoradiotherapy plus surgery versus surgery alone for oesophageal or junctional cancer (CROSS): long-term results of a randomised controlled trial. *Lancet Oncol*. 2015;16:1090–1098. doi:10.1016/S1470-2045(15)00040-6
22. Johnson J, Thijssen B, McDermott U, et al. Targeting the RB-E2F pathway in breast cancer. *Oncogene*. 2016;35:4829–4835. doi:10.1038/onc.2016.32
23. Konagaya Y, Rosenthal D, Ratnayeke N, et al. An intermediate Rb-E2F activity state safeguards proliferation commitment. *Nature*. 2024;631:424–431. doi:10.1038/s41586-024-07554-2
24. Stepkowski SM, Chen W, Ross JA, et al. STAT3: an important regulator of multiple cytokine functions. *Transplantation*. 2008;85:1372–1377. doi:10.1097/TP.0b013e3181739d25
25. Yang PL, Liu LX, Li EM, et al. STAT3, the challenge for chemotherapeutic and radiotherapeutic efficacy. *Cancers*. 2020;12:2459. doi:10.3390/cancers12092459
26. Luo H, Yang Z, Zhang Q, et al. Carbon ion therapy inhibits esophageal squamous cell carcinoma metastasis by upregulating STAT3 through the JAK2/STAT3 signaling pathway. *Front Public Health*. 2020;8:579705. doi:10.3389/fpubh.2020.579705
27. Park SY, Lee CJ, Choi JH, et al. The JAK2/STAT3/CCND2 axis promotes colorectal cancer stem cell persistence and radioresistance. *J Exp Clin Cancer Res*. 2019;38:399. doi:10.1186/s13046-019-1405-7
28. Spitzner M, Ebner R, Wolff HA, et al. STAT3: a novel molecular mediator of resistance to chemoradiotherapy. *Cancers*. 2014;6:1986–2011. doi:10.3390/cancers6041986
29. Maranto C, Udhane V, Hoang DT, et al. STAT5A/B blockade sensitizes prostate cancer to radiation through Inhibition of RAD51 and DNA repair. *Clin Cancer Res*. 2018;24:1917–1931. doi:10.1158/1078-0432.CCR-17-2768
30. Qiu R, Chen W, Zhao S, et al. MAZ coordinates with HDAC1 to promote hepatocarcinoma proliferation and metastasis through transcriptional repression of CSK. *Mol, Carcinog*. 2025. doi:10.1002/mc.70005
31. Ma RJ, Ma C, Hu K, et al. Molecular mechanism, regulation, and therapeutic targeting of the STAT3 signaling pathway in esophageal cancer (Review). *Int J Oncol*. 2022;61:105. doi:10.3892/ijo.2022.5395
32. Leslie K, Lang C, Devgan G, et al. Cyclin D1 is transcriptionally regulated by and required for transformation by activated signal transducer and activator of transcription 3. *Cancer Res*. 2006;66:2544–2552. doi:10.1158/0008-5472.CAN-05-2203
33. Park JW, Han CR, Zhao L, et al. Inhibition of STAT3 activity delays obesity-induced thyroid carcinogenesis in a mouse model. *Endocr Relat Cancer*. 2016;23:53–63. doi:10.1530/ERC-15-0417
34. Sinibaldi D, Wharton W, Turkson J, et al. Induction of p21WAF1/CIP1 and cyclin D1 expression by the Src oncoprotein in mouse fibroblasts: role of activated STAT3 signaling. *Oncogene*. 2000;19:5419–5427. doi:10.1038/sj.onc.1203947
35. Kim H, Jo C, Jang BG, et al. Oncostatin M induces growth arrest of skeletal muscle cells in G1 phase by regulating cyclin D1 protein level. *Cell Signal*. 2008;20:120–129. doi:10.1016/j.cellsig.2007.09.004
36. Lindhorst E, Schumm-Draeger PM, Bojunga J, et al. Differences in tumor cell proliferation, HLA DR expression and lymphocytic infiltration in various types of thyroid carcinoma. *Exp Clin Endocrinol Diabetes*. 2002;110:27–31. doi:10.1055/s-2002-19991
37. WangC, LiZ, PanZ, et al.Rac1: a potential radiosensitization target of human nasopharyngeal carcinoma CNE2 cells. *Eur J Pharm Sci*. 2020;151:105378. doi:10.1016/j.ejps.2020.105378